

1N-05  
22324  
16P



# The Use of the Regier Number in the Structural Design With Flutter Constraints

H. J. Dunn and Robert V. Doggett, Jr.  
*Langley Research Center, Hampton, Virginia*

(NASA-TM-109128) THE USE OF THE  
REGIER NUMBER IN THE STRUCTURAL  
DESIGN WITH FLUTTER CONSTRAINTS  
(NASA. Langley Research Center)  
16 p

N95-11465

Unclass

G3/05 0022324

August 1994

National Aeronautics and  
Space Administration  
Langley Research Center  
Hampton, Virginia 23681-0001



## Summary

This preliminary investigation introduces the use of the Regier number as a flutter constraint criterion for aeroelastic structural optimization. Artificial Neural Network approximations are used to approximate the flutter criterion requirements as a function of the design Mach number and the parametric variables defining the aspect-ratio, center-of-gravity, taper ratio, mass ratio and pitch inertia of the wing. The presented approximations are simple enough to be used in the preliminary design stage without a well defined structural model. An example problem for a low-speed, high-aspect-ratio, light-aircraft wing is presented. The example problem is analyzed for the flutter Mach number using doublet lattice aerodynamics and the PK solution method. The use of the Regier number constraint criterion to optimize the example problem for minimum structural mass while maintaining a constant flutter Mach number is demonstrated.

## Introduction

The structural optimization of an airplane wing to satisfy flutter constraints is often an expensive process in terms of computer resource requirements. The typical iteration of the design through the optimization process requires repeated determination of the unsteady aerodynamic forces and subsequent flutter solutions. While the solution of the flutter equations requires little computer resources, the calculation of the unsteady aerodynamic forces often requires significant computer storage and central processor time. One means to reduce these costs, as discussed in references 1 and 2, is to use a simplified model of the unsteady aerodynamics. If the changes in the structure between adjacent iterations are small then the unsteady aerodynamic forces will be virtually unaffected and the aerodynamic model need not be updated at every iteration. A complete update might be made after, say, five iterations. Another simplified model, used in reference 3, assumes that the modal basis used to calculate the unsteady aerodynamic forces is unaffected during the optimization. This report presents an alternative approach to actually calculating the unsteady aerodynamic forces and explicitly solving the flutter equations during the optimization. The method uses a flutter criterion to evaluate the flutter susceptibility of the wing. Certain properties of the wing are compared with the criterion to assess whether or not the wing has acceptable flutter characteristics. The use of a flutter criterion is particularly attractive during preliminary design when a variety of wings are under study, and high accuracy is not required.

Although there are no flutter criteria that apply to all wings, there are criteria available that apply to many wings. For example, one flutter criterion is to

have the sectional center-of-gravity forward of the sectional aerodynamic center-of-pressure. However when this criterion is used for the design of a wing, the resulting design has excessive weight. The criterion for the flutter constraint used in this report is based on the stiffness-altitude parameter, or Regier number, which depends on the stiffness of the wing and characteristics of the fluid in which the wing is operating, in particular, the density and speed of sound. As the name stiffness-altitude implies, the value of the Regier number increases as either stiffness or altitude is increased. This parameter has been used in reference 4 to correlate the flutter results obtained from several hundred wind-tunnel, flutter-model tests.

The proposed criteria is "If the Regier number for the wing being designed is greater than a reference value, the wing is flutter free." The reference value is a calculated Regier number based on experimental flutter tests. If the Regier is substantially larger than the reference value, the wing has excess stiffness. This suggests that some material in the load bearing structure could be reduced (*i.e.* reduce the stiffness) and thus reduce the structural mass. If the Regier number is less than the reference value, then the wing will flutter. An advantage of the proposed criterion over other criterion is that this proposed criterion is easy to calculate and simple enough so that it may be used early in the design process.

The purpose of this paper is to discuss how a flutter constraint based on the Regier number can be used in optimizing an airplane wing. First the Regier number, including its background and meaning is introduced. This discussion is followed by the development of an artificial neural network (reference 5), or ANN, approximation for the reference Regier number data obtained from reference 4. Next, the procedure for using the Regier number in structural optimization is presented. Finally, the application of the Regier number criteria to an illustrative example is presented.

## Symbols

ANN	artificial neural network
$AR$	aspect ratio
$a$	speed of sound
$b = \frac{\bar{c}}{2}$	reference length, wing semichord
$\bar{c}$	mean aerodynamic chord
$C_{L\alpha}$	lift curve slope
$cg$	center of gravity, % $\bar{c}$
$ea$	elastic axis position, % $b$
$g$	constraint function used in CONMIN

$g$	structural damping coefficient	$y_j$	output of a neuron element (Equation 4)
$h_a, h_f$	height of aft or forward beam, Figure 8	$z$	vertical displacement of the beam at the typical wing section
$I$	input of ANN scaling function, (Equation 3)	$\omega$	frequency
$J$	objective function	$\mu = \frac{m}{\pi \rho b^2}$	mass ratio
$k$	reduced frequency	$\rho$	mass density of fluid
$K_{AR}$	ANN approximation for the $AR$ correction factor	$\rho_s$	mass density of the support structure
$K_{cg}$	ANN approximation for the $cg$ correction factor	$\Lambda$	sweep angle
$K_\lambda$	ANN approximation for the $\lambda$ correction factor	$\lambda$	taper ratio
$K_\mu$	ANN approximation for the $\mu$ correction factor	$\Theta_j$	bias parameter of neuron element (Equation 4)
$K_{r_\alpha}$	ANN approximation for the $r_\alpha$ correction factor	subscripts:	
$l$	semispan of wing	$\alpha$	pitch mode natural frequency
$M$	Mach number	$a$	aft beam
$m$	sectional wing mass	$\mathcal{C}$	conservative approximation
$O$	output of ANN scaling function, (Equation 7)	$d$	divergence condition
$p$	dummy argument of Equations 5 and 6	$\mathcal{E}$	best estimate approximation
$\mathcal{R} = \frac{\omega_r b}{a} \sqrt{\mu}$	Regier number	$f$	forward beam or flutter condition
$\bar{\mathcal{R}} = \frac{\mathcal{R}}{\sqrt{C_{L\alpha}}}$	Frueh's modified Regier number	$j$	$j^{th}$ neuron element
$\mathcal{R}^*$	Regier number approximation	$max$	maximum value
$r_\alpha$	radius of gyration, normalized by $b$	$min$	minimum value
$S_1, S_2$	Nonlinear transfer function used in ANN	$r$	reference
$t_a, h_f$	thickness of aft or forward beam wall, Figure 8	$0$	reference condition
$v$	vector of structural response variables	<b>The Regier Number</b>	
$V$	velocity	The Regier number, or stiffness-altitude parameter, is one of several nondimensional aeroelastic parameters that have been used to insure dynamic similarity between models (reference 6). The stiffness-altitude parameter was first suggested for use in displaying flutter data by Arthur A. Regier. Over time this parameter has become known as the Regier number, or $\mathcal{R}$ . The expression for $\mathcal{R}$ is	
$V_I = \frac{V}{b \omega_r \sqrt{\mu}}$	velocity index parameter	$\mathcal{R} = \frac{\omega_r b \sqrt{\mu}}{a} \quad (1)$	
$W$	beam mass per unit length	where $\omega_r$ is a reference frequency, $b$ is the reference length, $\mu$ is the mass ratio, and $a$ is the speed of sound. As is the case for the more familiar velocity index parameter <sup>1</sup> $V_I$ , $\mathcal{R}$ can be derived by simplifying	
$w_a, w_f$	width of aft or forward beam, Figure 8	<sup>1</sup> The velocity index parameter $V_I$ is related to $\mathcal{R}$ by the following relationship:	
$w_j$	weight parameter of neuron element (Equation 4)	$V_I = \frac{M}{\mathcal{R}}.$	
$Wt$	mass of the support structure		
$x$	vector of structural optimization design variables		

the approximate empirical flutter formula expression given by Theodorsen and Garrick in reference 7. A modified version of  $\mathcal{R}$  is presented by Frueh in reference 8. Frueh's modified Regier number  $\bar{\mathcal{R}}$  is given by

$$\bar{\mathcal{R}} = \frac{\mathcal{R}}{\sqrt{C_{L\alpha}}} \quad (2)$$

where  $C_{L\alpha}$  is the lift curve slope. This expression would be attractive for use in correlating flutter data because  $\bar{\mathcal{R}}$  has a smoother variation with Mach number than the Regier number does. However, in many instances  $C_{L\alpha}$  information is not available, especially from research flutter model tests, so it is often not possible to use  $\bar{\mathcal{R}}$ . It should be pointed out the Frueh's expression can also be derived from Theodorsen and Garrick's approximate empirical formula (reference 7) recognizing that  $C_{L\alpha}$  is  $2\pi$  in their formula. So, in effect, Regier's formulation essentially assumes a constant lift curve slope. Recent research reports since about 1970 have not often used either  $\mathcal{R}$  or  $V_I$  because these reports tend to be problem, or wing, specific. For a specific wing, presenting the stability boundary using  $\mathcal{R}$  or  $V_I$  is not as useful as a plot of the stability boundary using dynamic pressure. However, in aeroelastic research reports prior to the 1970's the focus of the research was in parametric studies and the presenting of the data using  $\mathcal{R}$  or  $V_I$  is very common.

$\mathcal{R}$  is also directly related to the parameters  $M$  and  $\mu$  that arise from a non-dimensional considerations of flutter. The term  $\frac{\omega_r b}{a}$  is the ratio of vibration velocity to fluid speed of sound and may be thought of as a modified Mach number. The remaining term  $\mu$  is the nondimensional ratio of mass of the body to the apparent mass of the fluid surrounding it.

In reference 6 Regier describes  $\mathcal{R}$  as the square root of the ratio between the structural inertia force and the fluid force at Mach 1. Using the Regier number to define the stability boundary stresses the importance of the ratio between the inertial forces and fluid forces as a primary factor in the governing equations of motion. Two dynamically similar models that have the same Regier number will have the same ratio of structural force to fluid forces at Mach 1. If the two models are also aerodynamically similar, then the flutter stability boundary will be the same when plotted in the  $\mathcal{R}$  vs  $M$  plane. Figure 1 shows  $\mathcal{R}$  plotted against Mach number for an typical wing. When constant dynamic pressure lines are plotted against  $M$ , they appear as radial lines through the origin as shown in Figure 1. The stable no flutter region is above the boundary; the unstable flutter region is below the boundary. Unlike  $V_I$ ,  $\mathcal{R}$  has the origin as an anchor point. The above properties makes  $\mathcal{R}$  an attractive parameter for correlating flutter data from different wing configurations.

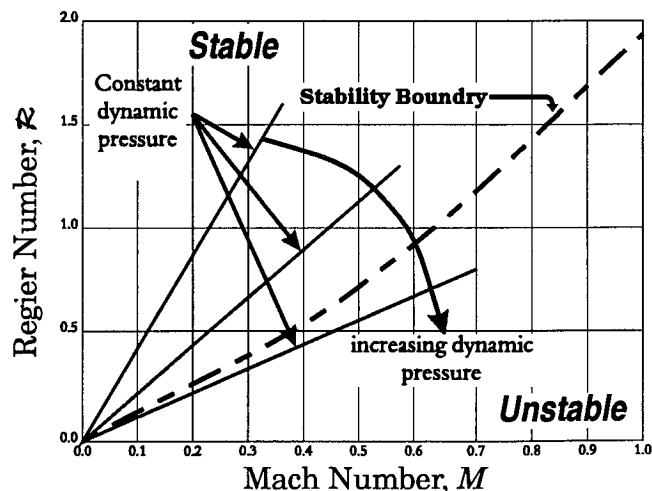


Figure 1. Regier Number Stability Plane.

For these reasons Harris (reference 4) chose  $\mathcal{R}$  to catalog flutter data from a variety of wing configurations. Reference 4 is a summary of 341 experimental and theoretical flutter studies presented as a series of flutter boundary plots of  $\mathcal{R}$  vs  $M$  and correction factors, such as the correction factor for the aspect ratio,  $K_{AR}$  vs  $AR$ . Figure 2 is a typical plot of  $\mathcal{R}$  vs  $M$  taken from reference 4 showing the flutter boundary and data points for low sweep conventional planform wings.

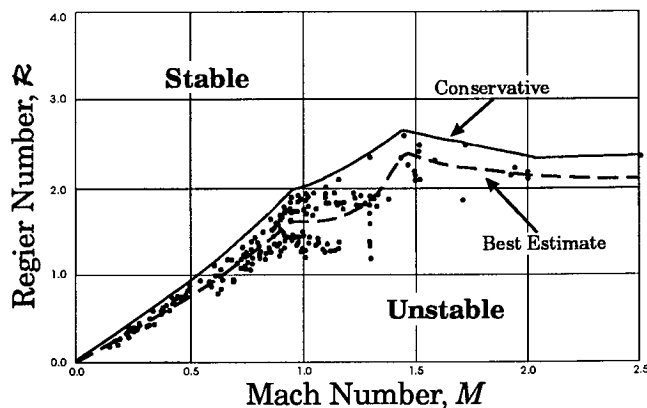


Figure 2. Regier Number vs Mach Number.

Other data plots in reference 4 are used for conventional planform wing of moderate and high sweep, and delta wing designs. The reference 4 designated "conservative estimate" and "best estimate" curves are shown in Figure 2 as solid and dashed lines, respectively. The conservative estimate curve encompasses all the experimental data whereas the best estimate curve is similar to a mean fairing though the data. The data in Figure 2 were adjusted by Harris to a nominal wing design for an average aspect ratio, center-of-gravity position, taper ratio, mass ratio, sweep angle, and radius of gyration. In practice, the data from reference 4 is adjusted for the particular  $AR$ ,  $cg$ ,  $\lambda$ ,  $\mu$ ,  $\Lambda$  and  $r_\alpha$  of the wing

design by using correction factors. The correction factors are normally a function of a single parameter with the exception of the correction factor for  $\mu$ . This will be explained in the "The Regier Number Approximation" section of the paper.

To determine if a wing design has an aeroelastic problem using reference 4, the  $\mathcal{R}$  of the design calculated using Equation 1 is compared to the adjusted  $\mathcal{R}$  value calculated by using the methods and data of reference 4. A flutter condition is predicted if the  $\mathcal{R}$  calculated using Equation 1 is less than the  $\mathcal{R}$  generated by using reference 4. If the  $\mathcal{R}$  of the design is greater than the  $\mathcal{R}$  of reference 4, then addition weight savings can be achieved by removing some of the structural mass being used to generate "excess" this stiffness.

## The Artificial Neural Network

Artificial neural networks (ANNs) are used in this report to approximate a number of curves in reference 4. This section serves to give the uninformed reader a brief introduction to the ANN. Further information on ANNs can be found in reference 5. ANNs are not unique to the work presented in this report and several other functions could have been used to approximate the data.

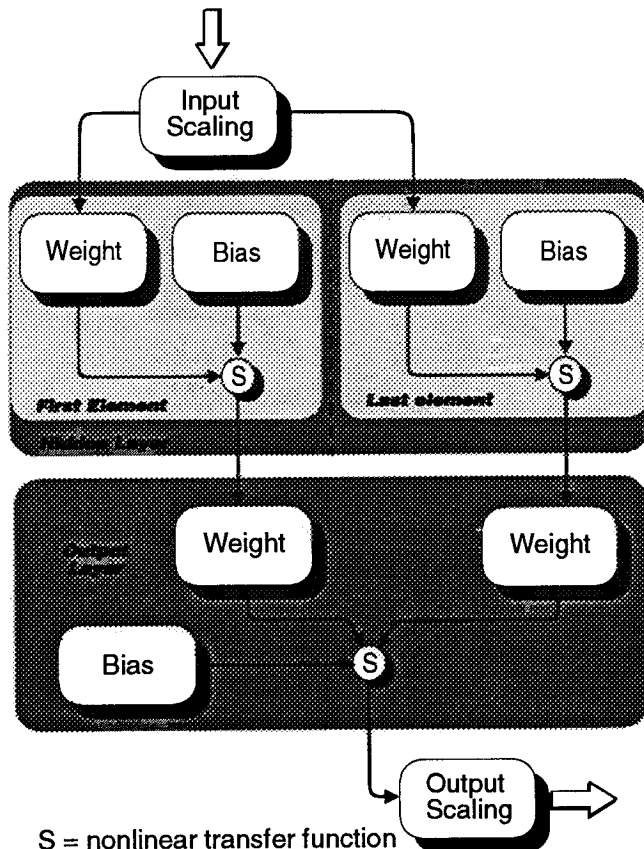


Figure 3. Artificial Neural Networks.

ANNs derive their name from trying to mimic the structure and functions of neural systems of living creatures. In general the network is composed of a number of signal processing elements, or artificial neurons. Figure 3 shows the form of the ANN using the McCulloch-Pitts neuron model (reference 5). In the conventional use of ANNs, the data is approximated by a single large ANN with several inputs and outputs. Because the data in reference 4 have been separated into several single input/output functions the conventional ANN model is not used. All of the ANNs developed in this report have a single input and output variable. The input variables are initially scaled before being passed to each neuron elements as shown in Figure 3. The individual neuron elements reside in what is commonly called the "hidden layer." The number of elements in the hidden layer determines the degree of accuracy of the approximation function. The more elements in the hidden layer the better the ANN is at approximating the original function. The output of each of the hidden layer elements is passed to the "output layer" which is also a neuron element. The output of the output layer is again scaled before being used.

The equations used for calculating the approximation are:

The input scaling function is

$$I_{scaled} = \frac{(I - I_{min})}{(I_{max} - I_{min})} * 0.8 + 0.1 \quad (3)$$

where  $I_{scaled}$  is the output of the scaling function, and  $I_{max}$  and  $I_{min}$  are the input scaling parameters.

The McCulloch-Pitts model for a single input neuron is described by

$$y_j = S_i (w_j I_{scaled} + \Theta_j) \quad (4)$$

where  $y_j$  is the output,  $w_j$  is the weight, and  $\Theta_j$  is the bias of the neuron element. The function  $S_i$  defines the type of limiting or nonlinear transfer function used in the neuron. The approximations generated in this report use the following two types of nonlinear transfer functions

$$S_1(p) = \frac{1 - e^{-2p}}{1 + e^{-2p}} \quad (5)$$

$$S_2(p) = \frac{1}{1 + e^{-p}} \quad (6)$$

where  $p$  is the input to the function. The same type of nonlinear transfer function is used for all neuron elements of a particular ANN approximation.

The output scaling function is

$$O = \frac{(y_j - O_{min})}{0.8} * (O_{max} - O_{min}) + O_{min} \quad (7)$$

where  $O$  is the output of the approximation,  $O_{max}$  and  $O_{min}$  are output scaling parameters, and  $y_j$  is given by equation 4. The parameters that define the ANN are the minimum and maximum of the input and output scaling functions plus the weights and biases of the each of the neurons elements. Equations 3 – 7 are used to approximate each of the individual functions that are joined together to form the Regier number approximation as described in the next section.

## The Regier Number Approximation

This section describes the approximations that are used to approximate the information contained in reference 4. Reference 4 presents the design estimates of the flutter margins as a series of basic flutter boundary plots in the form of  $\mathcal{R}$  vs  $M$  for wing configurations of specific values for  $AR$ ,  $cg$ ,  $\lambda$ ,  $\mu$ ,  $\Lambda$ , and  $r_\alpha$ . Parametric adjustment factors are presented as additional plots that are used to modify the basic boundary plots for variations in  $AR$ ,  $cg$ ,  $\lambda$ ,  $\mu$ ,  $\Lambda$ , and  $r_\alpha$ . These adjustment factors are necessary to account for wing configurations that are different from the base configuration. In Figure 4 the data and the ANN approximation function are shown for the aspect-ratio adjustment factor  $K_{AR}$  as a function of the wing aspect-ratio value  $AR$ . There are different basic flutter boundary plots for different planform designs, such as high sweep or delta platforms. The approximations calculated in this report for the base flutter boundary are for subsonic, low sweep, conventional-planform wing configurations.

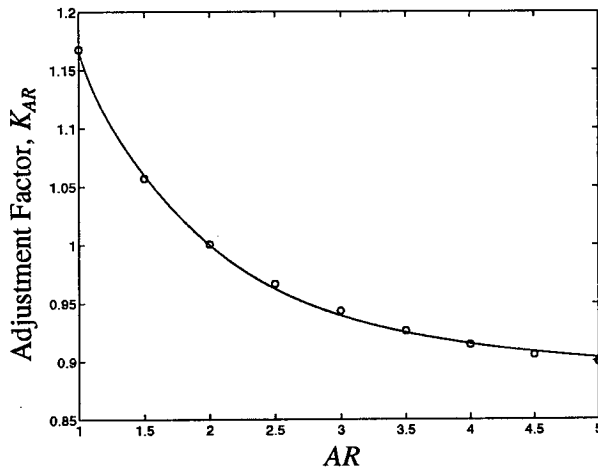


Figure 4. ANN Approximation of  $K_{AR}$ .

The  $K_{AR}$  ANN approximation function is calculated using Equation 7. The  $K_{AR}(AR)$  has a value of 1 for  $AR = 2$ , which represents the aspect-ratio value of the base configuration wing. There are four other adjustment factors,  $K_{cg}(cg)$  for the sectional wing cg

location,  $K_\lambda(\lambda)$  for the taper ratio,  $K_\mu(\mu, \Lambda, M)$  for mass ratio, and  $K_{r_\alpha}(r_\alpha)$  for the radius of gyration. Each of the adjustment factors are calculated using Equation 7. The mass ratio adjustment factor appears to be a function of  $\mu$ ,  $\Lambda$ , and  $M$  but it is actually only a function of  $\mu$ . The parameters  $\Lambda$  and  $M$  determine which one of 6 different functions of  $\mu$  is used. The complete ANN approximation for the flutter boundaries are:

$$\mathcal{R}_C^* = \frac{\mathcal{R}_C(M)}{K_{AR}(AR)K_{cg}(cg)K_\lambda(\lambda)K_\mu(\mu, \Lambda, M)K_{r_\alpha}(r_\alpha)} \quad (8)$$

$$\mathcal{R}_E^* = \frac{\mathcal{R}_E(M)}{K_{AR}(AR)K_{cg}(cg)K_\lambda(\lambda)K_\mu(\mu, \Lambda, M)K_{r_\alpha}(r_\alpha)} \quad (9)$$

where  $\mathcal{R}_C$  and  $\mathcal{R}_E$ , each calculated using Equation 7. The functions  $\mathcal{R}_C^*$ , equation 8, and  $\mathcal{R}_E^*$ , equation 9, are best and conservative estimate ANN approximations as a function of  $M$ ,  $AR$ ,  $cg$ ,  $\lambda$ ,  $\mu$ ,  $r_\alpha$ . The  $\mathcal{R}_C^*$  approximation is based on the envelope of  $\mathcal{R}$  whereas  $\mathcal{R}_E^*$  is based on the average value of  $\mathcal{R}$ .

Table 1 list the number elements in the hidden layer and the type of nonlinear transfer function (equations 5 or 6) used for each function. The value of zero for the  $K_{r_\alpha}$  entry of Table 1 denotes no hidden layer. Table 2 lists the function coefficients for the ANN approximations. Note that the coefficients for  $K_\mu$  entry of Table 1 is a single line in the table and is dependent on the value of  $\Lambda$  and  $M$  to determine which set of coefficients are used. As noted above and in Figure 3 each ANN has input and output scaling functions. Table 3 lists the scaling coefficients used in equations 3 and 7.

Equations 8 and 9 describe simple approximations that can be used with a minimum of computational effort to develop a constraint function for use in a complex structural optimization procedure or to check a design for its flutter margin.

Table 1. Regier ANN Configuration.

ANN function	Number of Elements in Hidden Layer	Nonlinear Transfer Function
$\mathcal{R}_E^*$	2	$S_1$
$\mathcal{R}_C^*$	2	$S_1$
$K_{AR}$	2	$S_2$
$K_{cg}$	2	$S_2$
$K_\lambda$	2	$S_2$
$K_\mu$	1	$S_2$
$K_{r_\alpha}$	0	$S_2$

Table 2. Regier ANN Coefficients.

Function	Hidden Layer		Output Layer	
	$w_j$	$\Theta_j$	$w_j$	$\Theta_j$
$K_{AR}$	-10.1802	6.4287	-2.8981	-0.2088
	11.3170	-1.6769	2.5877	
$K_{cg}$	-8.8731	4.6806	1.8229	-2.1408
	-12.3446	0.9841	5.6267	
$K_\lambda$	13.5425	-1.5790	-4.8732	2.6204
	-9.4929	4.8397	1.7489	
$K_\mu$ :				
$M < .9$				
$\Lambda < 20^\circ$	5.6802	-2.1022	-1.4161	0.6581
$20^\circ < \Lambda < 52^\circ$	-6.1022	1.4173	2.7400	-1.0061
$\Lambda > 52^\circ$	6.0479	-1.1682	-3.4544	2.3473
$M > .9$				
$\Lambda < 20^\circ$	-6.2028	1.0579	2.7628	-0.8023
$20^\circ < \Lambda < 52^\circ$	6.3106	-0.8072	-5.0643	3.8784
$\Lambda > 52^\circ$	5.3574	0.6696	7.5510	-2.0054
$K_{r_\alpha}$			5.6931	-2.8362
$\mathcal{R}_C^*$	-1.3377	-1.1461	-0.3777	0.6175
	1.4409	-1.2542	0.4905	
$\mathcal{R}_E^*$	1.3996	-0.5984	0.3697	0.7787
	1.3784	-1.0410	0.1003	

Table 3. Regier ANN Scale factors.

Function	Input		Output	
	Max	Min	Max	Min
$K_{AR}$	2	.2	1.5000	0.8993
$K_{cg}$	60	35	1.7877	0.8098
$K_\lambda$	1	0	2.2616	0.9048
$K_\mu$	90	10	1.2390	0.7512
$K_{r_\alpha}$	0.7	0.3	1.2630	0.7321
$\mathcal{R}_C^*$	1.8226	0	6	-6
$\mathcal{R}_E^*$	2.6731	0	6	-6

## Structural Optimization Using the Regier Number Constraint

This section describes the use of the ANN approximation of the Regier number  $\mathcal{R}^*$  in a structural optimization procedure for the design of flutter free wing while minimizing

$$J = Wt \quad (10)$$

where  $J$  is the objective function and  $Wt$  is the mass of the support structure. Figure 5 shows the design optimization procedure used in this report. The procedure consists of two major independent computer pro-

grams. These are a MSC/NASTRAN<sup>®2</sup> finite-element and sensitivity analysis program (reference 9) and, a second program denoted as **Optimizer** in Figure 5. The MSC/NASTRAN<sup>®</sup> analysis, denoted as (**Sensitivity & FEM Analysis**), uses a finite-element model (**FEM**) to generate the coefficients of the sensitivity equations. The **Optimizer** program calculates the objective function  $J$ , the gradient of the objective function  $\frac{\partial J}{\partial x}$ , and the constraint function  $g$ , for the optimization program CONMIN (reference 10). The CONMIN program is only used to solve the linear optimization problem. The design variable equations that are generated by MSC/NASTRAN<sup>®</sup> have the form

$$v = v_0 + \frac{\partial v}{\partial x}(x - x_0). \quad (11)$$

where  $v$  is a vector of structural design responses,  $v_0$  is the value of the design responses at the start of the optimization step,  $\frac{\partial v}{\partial x}$  is a matrix of sensitivity coefficients,  $x_0$  is a vector of the value of the design variables at the start of the CONMIN optimization, and  $x$  is a vector of design variables used in CONMIN. The structural response vector  $v$  are functions that are computed within the MSC/NASTRAN<sup>®</sup> program. These responses can include weight, displacements due to specified load conditions, stress, and modal frequencies, etc. The elements of the design variable  $x$  are problem dependent and may include plate thickness, beam height, and flange width, etc. The matrix  $\frac{\partial v}{\partial x}$  is computed by MSC/NASTRAN<sup>®</sup> using a finite-difference scheme. The sensitivities are transferred to the structural optimization program **Optimizer** as shown in Figure 5 and in more detail in Figure 6. Figure 6 shows the **Optimizer**'s internal flow as it cycles in the design space requiring the calculation of the objective function and constraint, or gradients of the objective function and constraint. As shown in Figure 6, the **Optimizer** program supplies the CONMIN program with the value of the objective function  $J$ , the constraint  $g$ , or the gradients of the objective function  $\frac{\partial J}{\partial x}$ . The CONMIN program calculates the gradient of  $g$  by using a finite-difference scheme.

The **Optimizer** finds the value of the design variable  $x$  that minimizes the linear cost function of Equation 10 subject to a non-linear inequality constraint

$$\mathcal{R}^* - \mathcal{R} < 0 \quad (12)$$

where  $\mathcal{R}$  is Regier number calculated using Equation 1, and  $\mathcal{R}^*$  is the required Regier number calculated from

<sup>2</sup> MSC/ is a registered trademark of The MacNeal-Schwendler Corporation. NASTRAN is a registered trademark of the National Aeronautics and Space Administration.



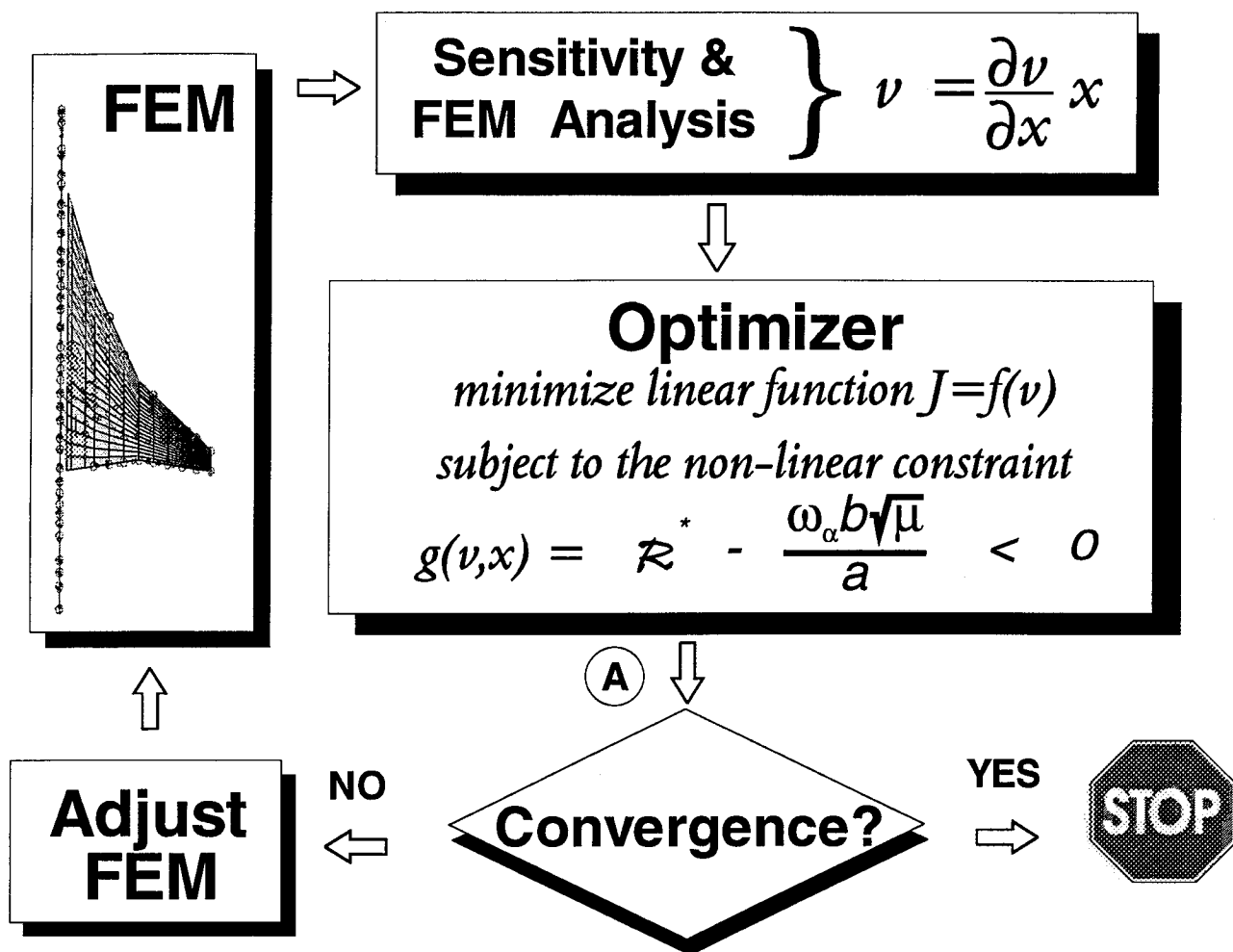


Figure 5. Design Optimization Iteration Procedure.

either Equation 8 or 9. Hereafter Equation 12 will be referred to as the Regier design constraint.  $\mathcal{R}$  is calculated using Equation 1 from the modal frequency  $\omega_r$ , the wing mass  $m$ , constants dependent on the flight condition  $\rho$  and  $a$ , and if the shape optimization is being done, grid point locations of the **FEM**. The approximation  $\mathcal{R}^*$  is calculated using either Equations 8 or 9, and is a function of the independent variables  $AR$ ,  $cg$ ,  $\lambda$ ,  $\Lambda$ ,  $\mu$ ,  $r_\alpha$  and  $M$ . With the exception of  $\rho$  and  $M$ , all of the independent variables for calculating  $\mathcal{R}$  and  $\mathcal{R}^*$  must be calculated from the vectors  $v$  and  $x$ . The calculation of the Regier constraint from the vectors  $v$  and  $x$  is illustrated in the sample problem discussed in the next section. The values of  $\rho$  and  $M$  must be specified by the user. The CONMIN optimization program finds the value of  $x$  which will minimize the cost function, usually structural weight, subject to the Regier constraint defined by Equation 12.

A complete design iteration is a single pass around the path shown in Figure 5, executing the **Sensitivity & FEM Analysis** and **Optimizer** programs once. At the end of the CONMIN optimization program, the

design responses calculated with Equation 12 will not agree with the value calculated with the FEM analysis unless the two systems have converged. The design optimization procedure, Figure 5, must iterate between the **Sensitivity & FEM Analysis** program and the **Optimizer** program until the design responses agree, or converge. A converged design is defined when the objective function and the design variables do not change during a design iteration. The reason for the disagreement between the CONMIN and MSC/NASTRAN® design responses is that the **Sensitivity & FEM Analysis** program is calculating the responses using a nonlinear FEM of the structure and the **Optimizer** program is using a model of the structure linearized about the initial value of the design variables. At the end of the CONMIN optimization step the new values of the design responses of the linear model may not agree with the responses of the nonlinear model at the optimized value of the design variables. This behavior can be seen in the results of the sample problem in the next section. If the design has not converged, a MSC/NASTRAN® analysis is done using a new FEM based on the new

value of  $x$  and the optimization of the linear structural model is repeated. The design optimization procedure is repeated until the design responses of the sensitivity analysis agree with the value of the design response calculated with MSC/NASTRAN®, as shown in Figure 5.

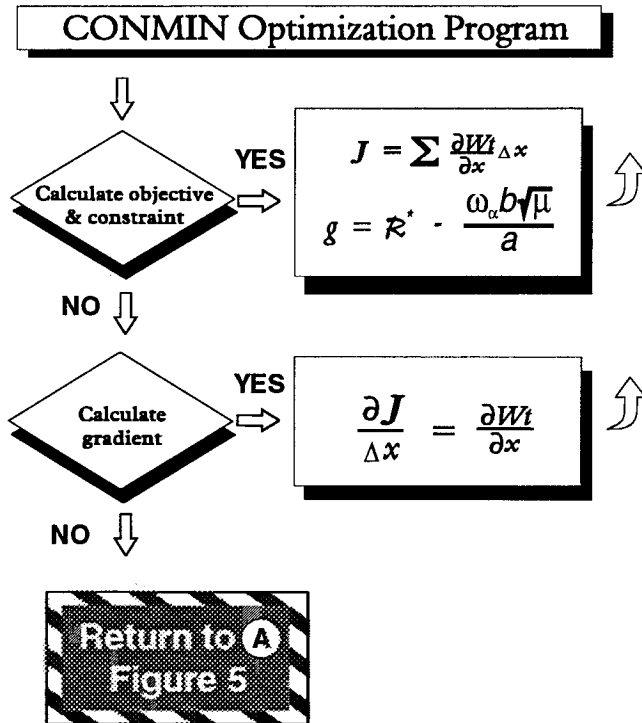


Figure 6. CONMIN Optimization Program.

## Example Problem Definition, Analysis, and Optimization Results

This section describes an example problem for demonstrating the use of the Regier number constraint in the optimal design of a wing subject to a flutter requirement. The example was chosen to be complex enough to represent an actual aircraft wing. The following model specifications were selected *a priori*:

1. Shape optimization will not be done.
2. The wing will have a high  $AR$ ,  $AR > 5$ .
3. The wing will be untapered,  $\lambda = 1$ .
4. The flow regime will be subsonic, and  $\Lambda = 0$ . The optimization will be for sea level flight condition.
5. The support structure will be two simple beams.
6. The dimensions and mass balance of the wing will be that of a typical light airplane wing that is in agreement with items 2 – 5 and designed to flutter at a subsonic  $M$ .

As a result of the above specifications  $R^*$  is a function of  $M$ ,  $\mu$ ,  $r_\alpha$  and  $cg$ . The optimization problem will be to design a minimum mass structure. The design

Mach number is the flutter Mach number of the initial wing design.

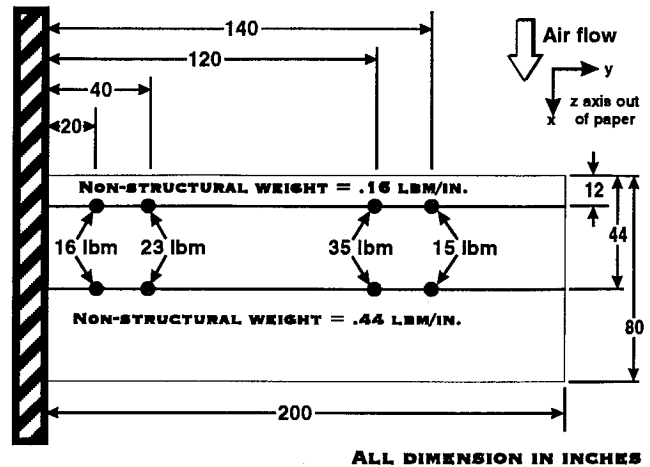


Figure 7. Example Problem: Wing Planform.

## Structural Model

The planform of the example wing is presented in Figure 7. The wing is rectangular in shape with a semispan and chord of 200 and 80 in., respectively. The structure of the wing is modeled as two uniform cantilever beams. The forward and aft beam locations are placed at  $0.15\bar{c}$  and  $0.55\bar{c}$  to represent a typical wing box structure.

Each beam is modeled with 10 beam elements. The wing is constrained so that the aft beam is connect to the forward beam by rigid links. The forward beam is free to displace vertically and twist about its long axis. Each beam is carrying an amount of non-structural distributed mass that is proportional to the cross-sectional area from the the point midway between the beams to the leading or trailing edge of the wing. The forward beam has 0.16 lbm/in., and the aft beam has 0.44 lbm/in. of non-structural mass. To simulate the landing gear, concentrated masses of 16 and 23 lbm are located respectively on each beam at 20 and 40 in. span stations. To simulate fuel, concentrated masses of 35 and 15 lbm are located respectively on each beam at 120 and 140 in. span locations. In Figure 7, these concentrated masses are represented by small circles on each beam. Initial mass and balance information for the example wing are given in Table 4.

The design variables for the forward and aft beams are height  $h_f$  and  $h_a$ , width  $w_f$  and  $w_a$ , and wall thickness  $t_f$  and  $t_a$  of the rectangular beam section as shown in Figure 8. Table 5 summarizes the lower bound, initial, and upper bound values of the design variables.

Table 4. Example Problem: Wing Weights and Balances.

Element	Structural Mass(lbm)	Non-structural Mass(lbm)	Total Mass(lbm)
Forward Beam	23.2	32	55.2
Aft Beam	23.2	88	111.2
Fuel		100	100
Landing Gear		78	78
<b>Total</b>	<b>46.4</b>	<b>298</b>	<b>344.4</b>

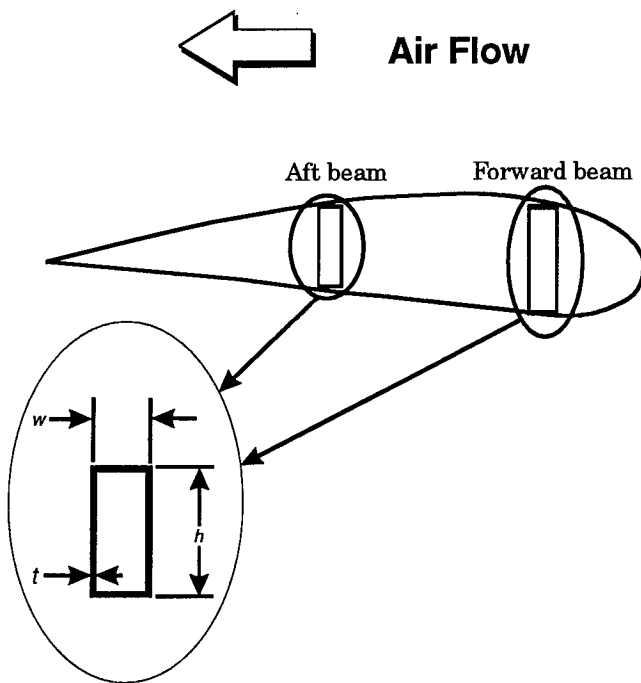


Figure 8. Example Problem: Wing Cross Section.

Table 5. Example Problem: Wing Design Parameter Values.

Parameter	Lower Bound (in.)	Initial Value (in.)	Upper Bound (in.)
$w_f$	1	2	3
$h_f$	2	4	5
$t_f$	0.05	0.1	0.2
$w_a$	1	2	3
$h_a$	2	4	5
$t_a$	0.05	0.1	0.2

### Flutter Analysis

To determine the flutter Mach number design value, and to check the accuracy of the Regier constraint

criterion, a separate flutter analysis is conducted at each optimization iteration. The flutter analysis is in no way a required step in the optimization procedure. The flutter Mach number  $M_f$  for the initial wing will define the  $M$  for the design calculations. This section gives the details of how the flutter speed is calculated using the MSC/NASTRAN® computer program.

The first four vibration modes are used for the aeroelastic equations of motion. The vibration analysis results for these modes are presented in Table 6 and Figure 9. The first mode, 17 Hz, is the first bending mode. The second mode, 21 Hz, is the first torsion mode. The third mode, 46 Hz, is the second bending mode. The fourth mode, 58 Hz, is the second torsion mode. Both bending modes have significant amounts of torsion due to coupling between the plunge and pitch motion of the wing.

Table 6. Example Problem: Wing Vibration Analysis.

Mode	Frequency (Hz)	Generalized Mass	Generalized Stiffness
1 <sup>st</sup> bending	17	$2.829 \times 10^1$	$3.271 \times 10^5$
1 <sup>st</sup> torsion	21	$1.769 \times 10^{-1}$	$3.090 \times 10^3$
2 <sup>nd</sup> bending	46	$1.350 \times 10^1$	$1.121 \times 10^6$
2 <sup>nd</sup> torsion	58	$6.760 \times 10^{-2}$	$8.980 \times 10^3$

The unsteady aerodynamics are calculated using the doublet lattice method (reference 12). The aerodynamics planform, Figure 7, is divided into 10 spanwise and 5 chordwise aerodynamic boxes for the double lattice procedure. Beam spline (reference 11) interpolation is used to calculate the aerodynamic grid deflection from the motion of the forward beam. Unsteady generalized aerodynamics forces, GAFs, are calculated for the values of reduced frequency  $k = [0.001, 0.1, 0.2, 0.3, 0.4, 0.5, 0.6, 0.7, 1, 5]$  and  $M = [0.3, 0.6]$ . Linear interpolation is used to calculate the GAFs at intervening values of  $k$  and  $M$ . The PK solution method, reference 11, is used to solve the dynamic equations of motion at  $V = 600$  to 12000 in./sec in increments of 600 in./sec and  $M = [0, 0.2, 0.3, 0.4, 0.5, 0.6]$ . Figure 10 presents a typical results of a PK analysis for  $M = 0.4$  for the above structural model with the design variables at their initial values. The data in Figure 10 indicates the 1<sup>st</sup> wing torsion mode going unstable at  $V = 5000$  in./sec ( $M=0.37$ ),  $\omega = 19.5$  Hz and 1<sup>st</sup> wing bending mode diverging at  $V = 9100$  in./sec, ( $M=0.67$ ). Note, that the predicated  $M$  for the data in Figure 10 is less than the specified  $M$  for the calculated GAF data. The true instability point, often referred to as the "match point", is found by interpolating the data in Figure 10 with other results from the PK solution method ( $M =$

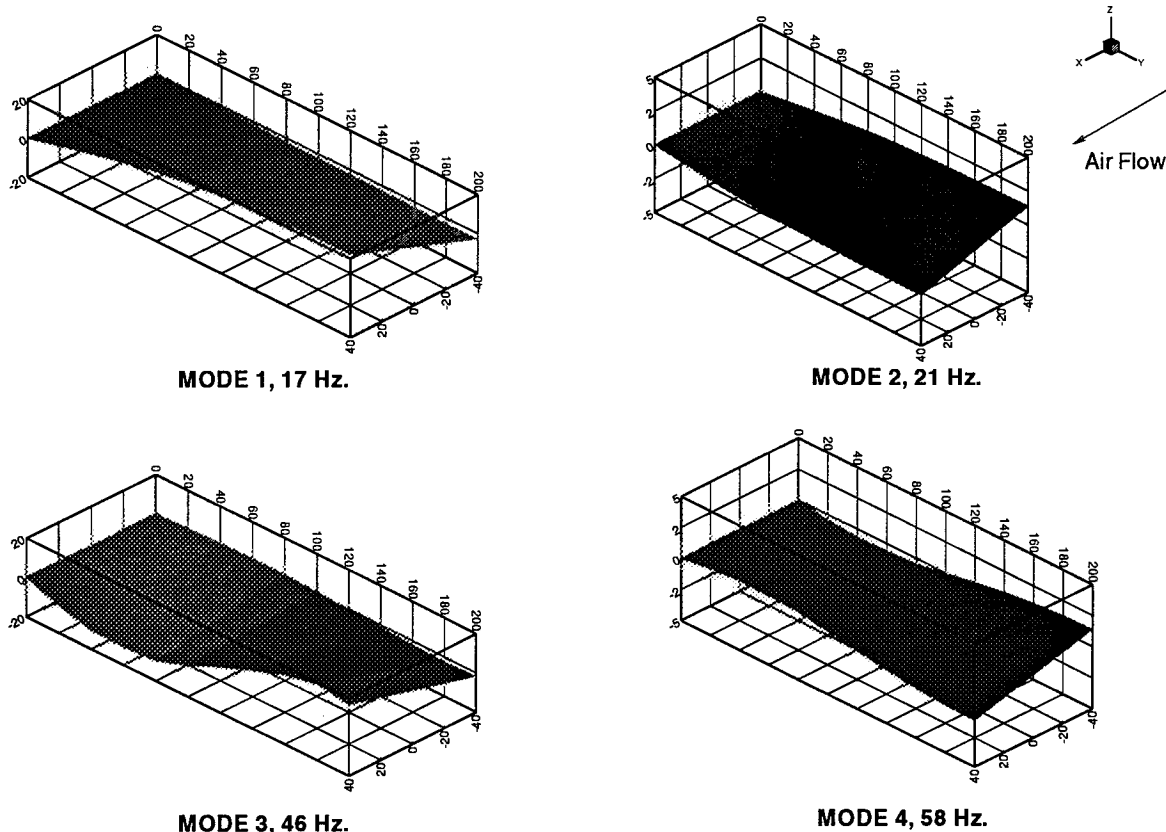


Figure 9. Example Problem: Vibration Modes.

0.3). The interpolated match point, or stability condition where  $\rho$ ,  $M$ , and  $V$  are in agreement for a standard atmosphere, is  $V_f = 5030$  in./sec ( $M_f = 0.37$ ), at  $\omega_f = 19.5$  Hz and  $V_d = 8590$  in./sec ( $M_d = 0.63$ ).

### Regier Constraint Calculation

The Regier constraint for use in the **Optimizer**, (Figures 5 and 6), is developed in this section. The elements of the vector  $v$  in Equation 11 for this example are the variables  $Wt$ ,  $\omega_\alpha$ ,  $z_a$  and  $z_f$ . The required parameters in Equations 8 or 9 for the calculation of the  $\mathcal{R}^*$  are  $M$ ,  $\mu$ ,  $r_\alpha$ , and  $cg$ . The purpose of this section is show how the these variables are calculated from the vector  $v$ . During the CONMIN optimization calculations, the design responses are approximated using Equation 11. For example, the deflection of the aft beam  $z_a$  is approximated by

$$z_a = z_{a0} + \frac{\partial z_a}{\partial x}(x - x_0) \quad (13)$$

where  $z_{a0}$  is the value of the aft beam at the start of the CONMIN program.

The Regier database in reference 4 is based on the sectional wing characteristics at the 75 percent span

location. For this example problem the nearest grid locations occur at the 80 percent span location and these grid locations are used to calculate  $\mu$ ,  $r_\alpha$ , and  $cg$ . The 80 percent span was used because for this problem the parameters  $\mu$ ,  $r_\alpha$ , and  $cg$  do not change between the 75 percent and 80 percent span locations.

The mass ratio for the example wing is

$$\mu = \frac{Wt + 0.6l}{\pi lb^2 \rho} \quad (14)$$

where  $Wt$  is the mass of the support structure,  $l$  is the semispan of the wing,  $b$  is the wing semichord, and  $\rho$  is the density of the fluid. Note that this expression for  $\mu$  contains the mass of the beams and the nonstructural mass, but does not contain the mass of the landing gear or fuel. For the values of  $l=200$  in.,  $b=40$  in. and  $\rho = 1.39 \times 10^{-4}$  lbm/in.<sup>3</sup> Equation 14 becomes

$$\mu = \frac{Wt + 120}{44.59} \quad (15)$$

For the initial wing design  $\mu = 3.69$ .

The center-of-gravity  $cg$  is calculated by using

$$cg = \left( 0.5 + \frac{0.05(W_a + 0.44) - 0.35(W_f + 0.16)}{W_a + W_f + 0.6} \right) \times 100 \quad (16)$$

where the sectional mass of the beams  $W_a$  and  $W_f$  are calculated by using

$$W_x = \rho_s (2t_x(h_x + w_x) - 4t_x^2) \quad (17)$$

where  $\rho_s$  is the mass density of the support structure, and the subscript  $x$  is either  $a$  or  $f$  to denote the aft or forward beam. For the initial wing design  $cg = 41.8$ .

The radius of gyration  $r_\alpha$  parameter is calculated by using

$$r_\alpha = \sqrt{\frac{(W_a + 0.44)(0.1 - ea)^2 + (W_f + 0.16)(0.7 - ea)^2}{W_a + W_f + 0.6}} \quad (18)$$

where  $ea$  is calculated by using the displacements  $z_f$  and  $z_a$  due to a torque applied to the wing tip. That is,

$$ea = 0.1 - 0.8 \frac{z_a}{z_a + z_f} \quad (19)$$

For the initial wing design  $r_\alpha = 0.4$ .

Figure 11 shows  $\mathcal{R}_c^*$  and  $\mathcal{R}_\varepsilon^*$  as a function of  $M$  and the flutter analysis result (solid circle symbol) for the initial wing design. The data in Figure 11 indicate that the  $\mathcal{R}_\varepsilon^*$  is a sufficiently accurate to be used in Equation 12 for  $\mathcal{R}$ . That is, the approximation of "best estimate" stability boundary is essentially the same as the doublet lattice calculated stability boundary. Substituting Equations 1 for  $\mathcal{R}$  and 9 for  $\mathcal{R}^*$  into Equation 12, with  $K_{AR}(5) = 0.9029$ ,  $K_\lambda(1) = 0.9028$ , and  $a = 13587$  in./sec yields the Regier constraint for an unswept wing with  $AR=5$  and  $\lambda=1$  as a function  $M$ ,  $cg$ ,  $\mu$ , and  $r_\alpha$ :

$$\frac{1.227\mathcal{R}_\varepsilon^*(M)}{K_\mu(\mu)K_{cg}(cg)K_{r_\alpha}(r_\alpha)} - \frac{\omega_\alpha\sqrt{\mu}}{340} < 0 \quad (20)$$

where  $K_\mu(\mu)$  represents the  $K_\mu$  adjustment factor approximation for  $M < .9$  and  $\Lambda < 20^\circ$ .

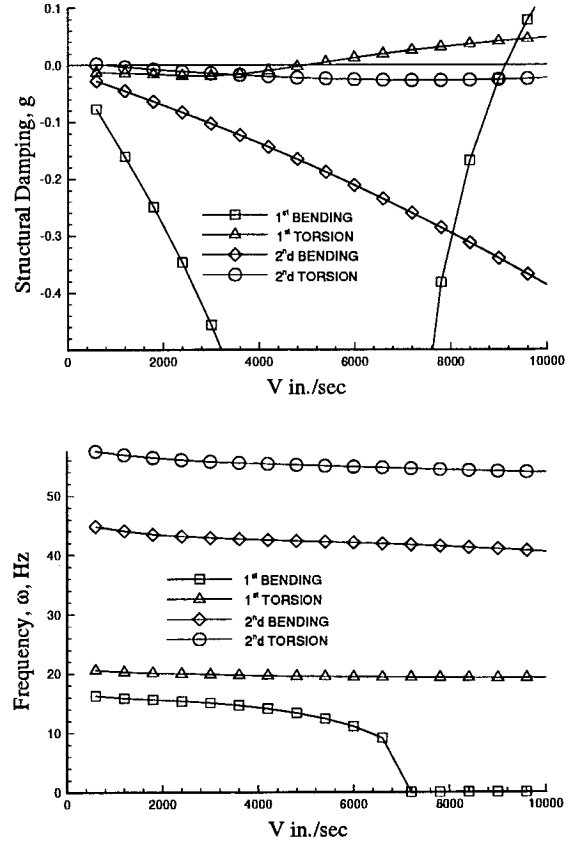


Figure 10. Example Problem: Aeroelastic Analysis.

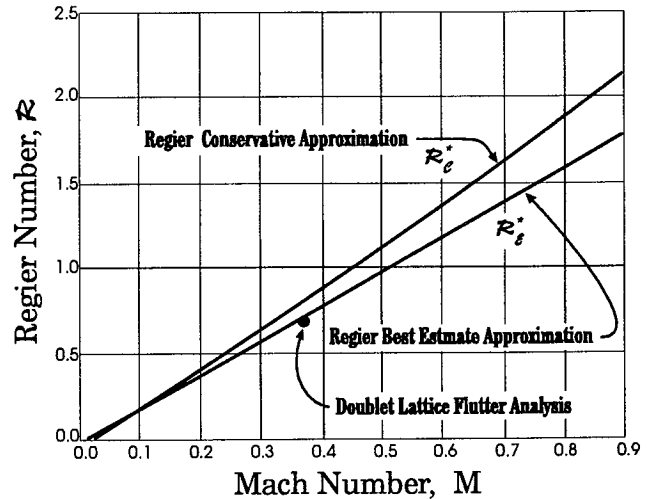


Figure 11. Example Problem: Regier Constraint Function.

## Structural Optimization Results

The doublet lattice analysis predicts the initial example wing to flutter at  $M = 0.37$ . The objective of the optimization is to design a minimum mass wing (i.e. minimize  $Wt$ ) that will be flutter free at  $M = 0.37$ . For

$M = 0.37$  and  $\mathcal{R}_{\mathcal{E}}^* = 0.621$  Equation 20 becomes

$$\frac{0.763}{K_{\mu}(\mu)K_{cg}(cg)K_{r\alpha}(r_{\alpha})} - \frac{\omega_{\alpha}\sqrt{\mu}}{340} < 0 \quad (21)$$

The design variable vector  $x$  in Equation 11 consists of the six variables  $w_a$ ,  $w_f$ ,  $h_a$ ,  $h_f$ ,  $t_a$ , and  $t_f$ . CONMIN's solution to the problem is to set all of the design variables, except  $h_f$ , to the lower design variable bounds and to find the value of  $h_f$  that satisfies the constraint function defined by Equation 21. Figure 12 is the optimization history for the design variable  $h_f$  and Table 7 lists the values of the design variables for the converged design. Figure 13 shows the optimization history of  $Wt$ . The final value of  $Wt$  is 16.6 lbm, a reduction of 29.8 lbm.

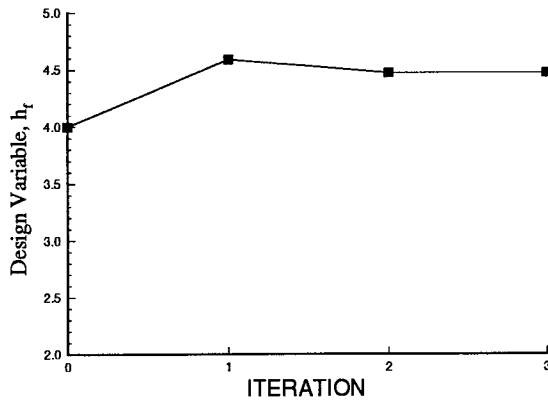


Figure 12. Optimization Results:  $h_f$  vs Iteration.

Table 7. Example Problem: Final Wing Design Variables Values.

Design Variable	Final Value (in.)
$w_f$	1
$h_f$	4.474
$t_f$	.05
$w_a$	1
$h_a$	2
$t_a$	.05

For the first and second optimization iterations in Figure 13 the discontinuous nature of the structural optimization results is quite noticeable. The first and second optimization iterations are bounded by the  $\square$  and  $\Delta$  symbols. Convergence at the end of iteration 2 between the linear optimization equations and the finite element analysis equations is indicated in Figure 13 by the symbol  $\nabla$ , designating the third CONMIN

optimization step, combining with the symbol  $\Delta$ , designating the second CONMIN optimization step, to give the appearance of the symbol  $\star$ .

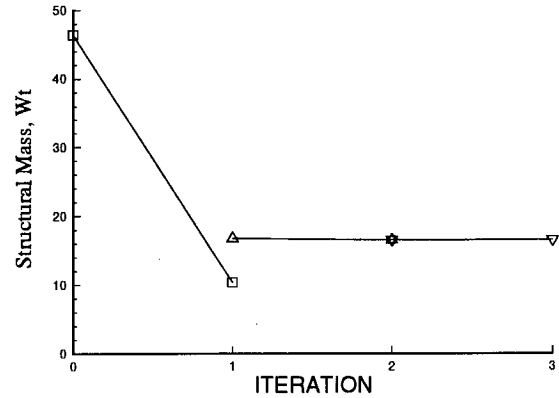


Figure 13. Optimization Results: Structure Mass vs Iteration.

Figure 14 presents the history of the  $\mathcal{R}$  and  $\mathcal{R}_{\mathcal{E}}^*$  terms of the constraint function during the optimization. The solid line in Figure 14 is  $\mathcal{R}$  and the dotted line is  $\mathcal{R}_{\mathcal{E}}^*$ . Equation 20 is satisfied in Figure 14 whenever the solid line is above the dotted line. At the beginning of the first iteration, denoted as iteration 0 in Figure 14, the data indicates that the structure has excess stiffness because  $\mathcal{R} > \mathcal{R}_{\mathcal{E}}^*$ . During the first CONMIN optimization step, *i.e.* between iterations 0 and 1 in Figures 12 – 14, the smallest  $h_f$  is found that satisfies the nonlinear constraint described by Equation 20. The reduction structural mass is indicated in Figure 13. At the end of the CONMIN optimization step, the MSC/NASTRAN<sup>®</sup> analysis results are shown at iteration 1 in Figures 12 – 14. The new constraint function indicates that a further mass savings can be made by reducing the stiffness still further during the second CONMIN optimization step. The convergence of the optimization program in two iterations is confirmed by the third segment of the results being nearly flat in Figures 12 – 14.

In Figure 15 the flutter Mach number  $M_f$  predicted by the MSC/NASTRAN<sup>®</sup> flutter analysis is plotted against iteration number. The variation of  $M_f$  is considered to be within the accuracy of the calculation and the optimal design is considered to meet the design specifications. However, there is no guarantee that the optimal design will have the desired aeroelastic properties because the optimization only guarantees that  $\mathcal{R} > \mathcal{R}^*$ .

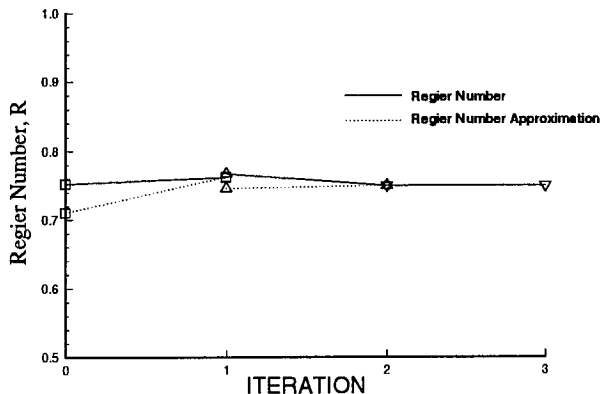


Figure 14. Optimization Results:  $\mathcal{R}$  and  $\mathcal{R}^*$  vs Iteration.

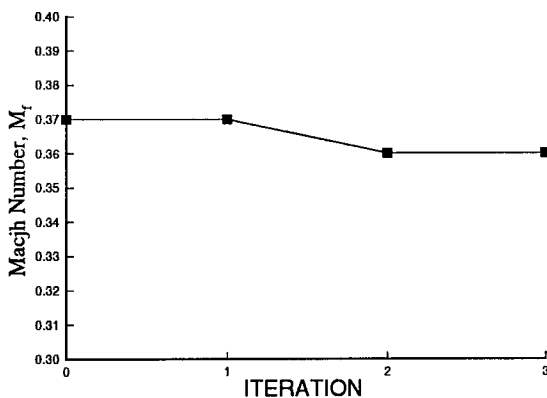


Figure 15. Optimization Results: MSC/NASTRAN® computed  $M_f$  vs Iteration.

Only a single initial value case is done in this paper because the objective of the paper is the examination of the Regier number criterion and not the optimization problem. If the structural optimization problem is of interest, several different initial conditions would have to be tested determine the existence of other minimum of the objective function in the design space.

Table 8 lists the execution times of the **Sensitivity & FEM Analysis**, **Optimizer** programs, and flutter analysis. The execution times listed in Table 8 are divided by the execution time of the flutter analysis program. Based on the data in Table 8, the Regier constraint is an efficient means for calculating an optimal structure with flutter constraint. The execution time for the structural optimization using the Regier constraint will be less than the procedure described in reference 3 since the method in reference 3 requires a calculations of the GAF at each iteration of the optimization.

Table 8. Example Problem: Program Execution Times.

Program	Relative Execution Time
Sensitivity Analysis	0.23
Optimizer	0.01
Aeroelastic Analysis	1.00

## Concluding Remarks

A flutter constraint criterion based on the Regier number for aeroelastic structural optimization is introduced. The use of a constraint criterion makes it unnecessary to calculate generalized unsteady aerodynamic forces between optimization cycles as do other methods used in aeroelastic design for flutter.

The application of the method proceeds in the following manner. Existing experimental flutter data in Regier number format are approximated by using Artificial Neural Networks. This approximation is then used to develop the flutter constraint criterion. Next, the optimal flutter acceptable wing design is achieved by adjusting the design parameters to achieve the minimum of the objective function, say structural weight, while satisfying the Regier constraint criterion.

The procedure is illustrated by the application to an example problem. A simple, rectangular wing is optimized for weight at a specified Mach number while achieving a desired minimum flutter condition. The data for developing the Regier number constraint are obtained from existing experimental results of similar configurations. The solution for the illustrative problem converged in two design cycles. Because of the simplicity of the Regier number approximation, little computer resources are required.

## References

1. Sobieszczanski-Sobieski, J.: Multidisciplinary Design Optimization: An Emerging New Engineering Discipline, *World Congress on Optimal Design of Structural Systems*, Rio de Janeiro, Brazil, August 2-6, 1993.
2. Chang, K. J.; Haftka, R. T.; Giles, G. L.; and Kao, P.-J.: Sensitivity Based Scaling for Correlating Structural Response from Different Analytical Models. AIAA Paper No. 91-925. Presented at AIAA/ASEM/ASCE/AHS/ASC 32nd Structures, Structural Dynamics, and Material Conference, Baltimore, MD, 1991.
3. Climent, Hector; and Johnson, Erwin H.: Aeroelastic Optimization Using MSC/NASTRAN, *International Forum on Aeroelasticity and Structural Dynamics*, May 22-26, 1993, Strasbourg, France.
4. Harris, G.: Flutter Criteria for Preliminary Design, Vought Aeronautics Report 2-53450/3R-467, September, 1963.

5. Cichocki, A.; and Unbehauen, R.: Neural Networks for Optimization and Signal Processing, John Wiley & Sons Ltd., 1993.
6. Regier, Arthur A.: The Use of Scaled Dynamic Models in Several Aerospace Vehicle Studies, *ASME Colloquium on the Use of Models and Scaling in Simulation of Shock and Vibration*, November 19, 1963, Philadelphia, Pennsylvania.
7. Theodorsen, Theodore; Garrick, I. E.: Mechanism of Flutter: T. R. No. 685, N. A. C. A., 1940.
8. Frueh, Frank J.: A Flutter Design Parameter to Supplement the Regier Number. *AIAA J.*, vol. 2, no. 7, July 1964.
9. Moore, Greg J.: MSC/NASTRAN Design Sensitivity and Optimization User's Guide, The MacNeal Schwendler Corp. April 1992.
10. Vanderplaats, Garret N.: CONMIN: A Fortran Program for Constrained Function Minimization User's Manual, NASA TM X 62-282, Ames Research Center and U.S. Army Air Mobility R&D Laboratory, Moffett Field, CA 94035.
11. Rodden, W. P.; Harder, R. L.; and Bellinger, E. D.: Aeroelastic Addition to NASTRAN, NASA CR 3094, March 1979.
12. Giesing, J. P.; Kalman, T.P.; Rodden, W. P.: Subsonic Unsteady Aerodynamics for General Configurations, Part II, Volume I - Application of the Doublet-Lattice Method and the Method of Images to Lifting-Surface/Body Interference, Air Force Flight Dynamics Laboratory Report No. AFFDL-TR-71-5, Part II, Vol. I, April 1972.





REPORT DOCUMENTATION PAGE			Form Approved OMB No. 0704-0188	
Public reporting burden for this collection of information is estimated to average 1 hour per response, including the time for reviewing instructions, searching existing data sources, gathering and maintaining the data needed, and completing and reviewing the collection of information. Send comments regarding this burden estimate or any other aspect of this collection of information, including suggestions for reducing this burden, to Washington Headquarters Services, Directorate for Information Operations and Reports, 1215 Jefferson Davis Highway, Suite 1204, Arlington, VA 22202-4302, and to the Office of Management and Budget, Paperwork Reduction Project (0704-0188), Washington, DC 20503.				
1. AGENCY USE ONLY (Leave blank)		2. REPORT DATE August 1994	3. REPORT TYPE AND DATES COVERED Technical Memorandum	
4. TITLE AND SUBTITLE The Use of the Regier Number in the Structural Design with Flutter Constraints			5. FUNDING NUMBERS WU 505-63-50-06	
6. AUTHOR(S) H. J. Dunn and Robert V. Doggett, Jr.				
7. PERFORMING ORGANIZATION NAME(S) AND ADDRESS(ES) NASA Langley Research Center Hampton, VA 23681-0001			8. PERFORMING ORGANIZATION REPORT NUMBER	
9. SPONSORING / MONITORING AGENCY NAME(S) AND ADDRESS(ES) National Aeronautics and Space Administration Washington, DC 20546-0001			10. SPONSORING / MONITORING AGENCY REPORT NUMBER NASA TM-109128	
11. SUPPLEMENTARY NOTES				
12a. DISTRIBUTION / AVAILABILITY STATEMENT  Unclassified - Unlimited  Subject Category 05			12b. DISTRIBUTION CODE	
13. ABSTRACT (Maximum 200 words)  This preliminary investigation introduces the use of the Regier number as a flutter constraint criterion for aeroelastic structural optimization. Artificial Neural Network approximations are used to approximate the flutter criterion requirements as a function of the design Mach number and the parametric variables defining the aspect-ratio, center-of-gravity, taper ratio, mass ratio and pitch inertia of the wing. The presented approximations are simple enough to be used in the preliminary design stage without a well defined structural model. An example problem for a low-speed, high-aspect-ratio, light-aircraft wing is presented. The example problem is analyzed for the flutter Mach number using doublet lattice aerodynamics and the PK solution method. The use of the Regier number constraint criterion to optimize the example problem for minimum structural mass while maintaining a constant flutter Mach number is demonstrated.				
14. SUBJECT TERMS Regier Number; Structural Optimization; Aeroelastic Vehicle Design; Flutter Design Constraint			15. NUMBER OF PAGES 15	
			16. PRICE CODE A03	
17. SECURITY CLASSIFICATION OF REPORT Unclassified	18. SECURITY CLASSIFICATION OF THIS PAGE Unclassified	19. SECURITY CLASSIFICATION OF ABSTRACT Unclassified	20. LIMITATION OF ABSTRACT	